

FUNCTIONAL-ORIENTED APPROACH FOR ANALYSIS OF PHYSICAL-MECHANICAL PROCESSES IN THE CUTTING ZONE

Alexandre Mikhailov¹, Elena Sydorova¹, Sergey Selivra²

¹Donetsk National Technical University, Department of Manufacturing Engineering,
58, Street Artiom, 83001 Donetsk, Ukraine

²Donetsk National Technical University, Department of Power-Mechanical Systems,
58, Street Artiom, 83001 Donetsk, Ukraine

Corresponding author: Elena Sydorova, sydorova@gmail.com

Abstract: Increase productivity in machining of hard materials, primarily associated with an increased strength of cutting tools. Cutting is accompanied by complex processes in different zones of contact of cutting tool and material. Therefore, to increase strength of the cutting tool is necessary to develop the technological actions in accordance with the peculiarities of the physico-mechanical processes in zones of cutting. The functionally-oriented approach solves this problem. However, obtaining information of physico-mechanical processes in different zones in cutting by experimentation is difficult by reason of the small contact zone of cutting tool and the material, high speed of process, problems with the installation of sensors and ensuring their accuracy, high cost of experiments. The development of thermo-mechanical cutting models solves this problem. The presented method was applied to increase the strength of carbide tools with TiAlN coating in the cutting of Ti6Al4V through analysis of thermo-mechanical model developed in Abaqus Explicit.

Key words: Cutting, Functionally-oriented approach, FEM, Ti6Al4V, Coating, TiAlN.

1. INTRODUCTION

Currently use hard materials in engineering is expensive, mainly due to the low productivity of their cutting related primarily to the low strength of cutting tools.

To increase the strength of the tool optimize cutting conditions, choose the structure and properties of the cutting tool, the cutting process is intensified by cutting fluids, laser technology, ultrasound, etc.

Incorrectly selected technological action can be not only ineffective, but also have a negative impact, therefore the problem studying of the processes in the cutting zone is actual.

Before, the study of methods for increasing resistance of cutting tools based on the experimental methods that require more material and time costs.

Currently, this problem is considered in terms of learning the physical and mechanical processes in the cutting zone, which are based on the thermo-mechanical model simulating the cutting process.

The different nature of loading requires a functional-oriented approach, which allows adapting the technological action for each zone of the tool. Analysis of the physico-mechanical processes in the cutting area is carried out by means of thermo-mechanical model of the cutting process.

Application of this technology is particularly effective for machining hard materials. For example of cutting titanium alloy Ti6Al4V by carbide tools with TiAlN PVD-coating, this method allowed to increase the cutting speed of 1.43 times without increasing the overall load on the cutting plate.

Further development of this technology provides for consideration of the factors at the macro-, meso- and micro levels, affecting the cutting process, as well as the introduction of technological action of various methods of intensification in the thermo-mechanical model.

2. GENERAL INFORMATION

2.1 Cutting conditions

This paper studies the cutting of titanium alloy Ti6Al4V by carbide tools with TiAlN PVD-coating and the geometry of ATI Stellram CNMG542A-4E SP0819 CNMG160608E-4E. Cutting conditions is presented in Table 1.

Table 1. Cutting conditions of Ti6Al4V

code	cutting speed, m/min	feed, mm/tr	depth, mm
vc65f03ae3	65	0.3	3
vc90f03ae3	90		
vc115f03ae3	115		

2.2 Creation of thermo-mechanical model to simulate the cutting process

Among the most popular software for the simulation of cutting by finite element method (Abaqus, Advantedge, Deform etc.), Abaqus interest in terms of openness of code and the possibility to integrate the various laws governing the behavior of materials

and their interactions. Thus, computer simulations have been implemented in the code Abaqus Explicit 6.10.

For the studies necessary to obtain the following information regarding the loading of the tool during cutting: contact pressure σ , contact shear τ , the contact temperature t . To obtain this information using the dynamic explicit analysis, type of the elements – coupled temperature-displacement.

To simulate the cutting process by finite element method use the Arbitrary Lagrangian-Eulerian approach (Pantalé, 1996), which largely avoids the problems associated with the degradation of the finite element mesh, as in the case of the Lagrangian approach.

Geometry, physical and mechanical properties of the cutting plate (the substrate and coating) and the material are embedded in the model.

Physical and mechanical properties of TiAlN coating and substrate WCCo6% are presented in Table 2.

Table 2. Physical and mechanical properties of TiAlN coating and substrate WCCo6%, (Jianxin et al., 2008; Gökkaya et al., 2009; Ozel et al., 2010; Okamoto et al., 2005; Staia et al., 2006; Kamnis et al., 2008; Kay et al., 2003)

parametres	substrate WCCo6%	TiAlN coating
density ρ , kg/m ³	14800	7400
Young's modulus E, GPa	560	600
Poisson's ratio, ν	0.23	0.20
thermal conductivity λ , W m ⁻¹ ·°C ⁻¹	55	22
specific heat c_p , J kg ⁻¹ K ⁻¹	295	480
thermal expansion α , mm·mm ⁻¹ ·°C ⁻¹	0.0000045	0.0000094

For the titanium alloy Ti6Al4V using functional temperature (t) dependencies (Ozel et al., 2010), (Chinmaya, et al., 2010), (Braham Bouchnak, 2010):

- Young's modulus E:

$$E(t)=0.7412 \cdot t+113375; \quad (1)$$

- thermal expansion α :

$$\alpha(t)=3 \cdot 10^{-9} \cdot t+7 \cdot 10^{-6}; \quad (2)$$

- thermal conductivity λ :

$$\lambda(t)=7.039 \cdot e^{0.0011 \cdot t}; \quad (3)$$

- specific heat c_p :

$$c_p=0.21 \cdot t+483.37 \text{ for } t \leq 1260\text{K}; \quad (4)$$

$$c_p=0.18 \cdot t+420.19 \text{ for } t > 1260\text{K}. \quad (5)$$

- density $\rho=4.42 \text{ kg/m}^3$;
- Poisson's ratio $\nu=0.342$.

The boundary conditions for finite element mesh and the material are shown in Fig. 1-2.

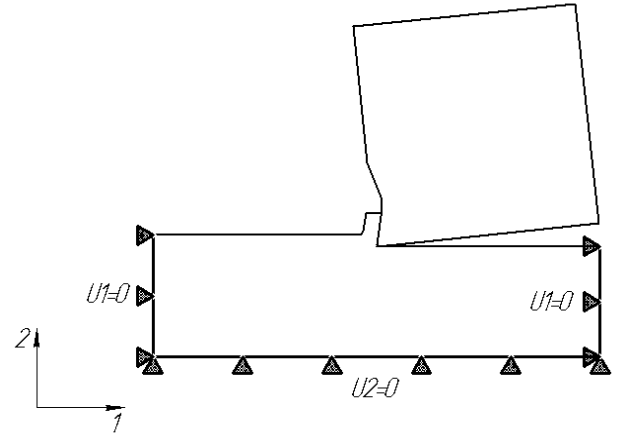


Fig. 1. The boundary conditions for finite element mesh

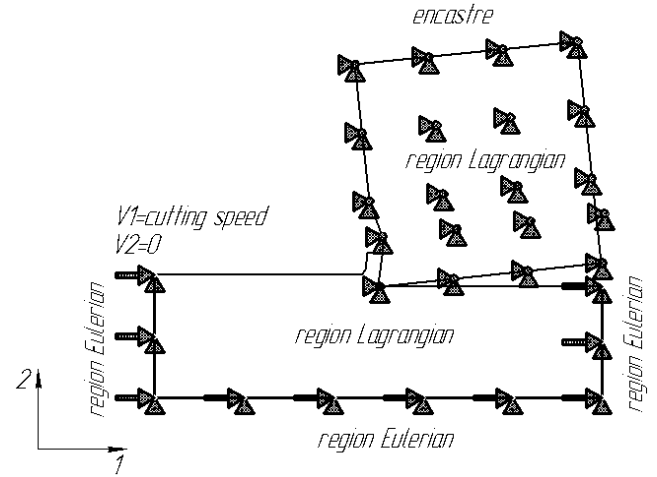


Fig. 2. The boundary conditions for the material

Among the various laws of material behavior at high strains, the most popular is Johnson-Cook law. It takes into consideration temperature gradients and the adiabatic shear phenomenon, caused by large plastic deformations.

This law establishes the dependence of stress σ on the degree of ε (%), strain rate and temperature T , and can be expanded in a multiplicative form for the three functions (Kalay, 2006):

$$\sigma = (A + B \cdot \varepsilon^n) \cdot \left(1 + C \cdot \ln \frac{\dot{\varepsilon}}{\dot{\varepsilon}_0}\right) \cdot \left(1 - \left[\frac{T - T_0}{T_f - T_0}\right]^m\right). \quad (6)$$

The first factor describes the phenomenon of work hardening, the second - the dynamic processes, the third - a phenomenon of drawing-back.

The factor associated with hardening, corresponds to the strain constant flow rate of deformation. A - the limit of elasticity of the material, B - the linear parameters of strain hardening, n - the nonlinear

parameters of strain hardening.

The second factor is a multiplicative factor describing dynamic hardening of the material. It depends of the speed of the equivalent plastic strain. C is a coefficient of sensitivity to strain rate.

The third factor is the factor corresponding to the phenomenon of heat drawing-back. T_0 - the initial temperature. Neglect the effect of temperature on the law of motion. For temperatures that are in the interval between T_0 and the melting temperature T_f , reduced strain movement with temperature and approach zero at $T = T_f$.

At temperatures tending to the melting point of strain movement is practically zero. Thus, T_0 is the temperature in relation to the mechanism which deals with heat drawing-back, and m – exponent of the heat drawing-back.

The coefficients of this law are obtained by tests on the static and dynamic torsion.

Parameters of the Johnson-Cook model for Ti6Al4V are presented in Table 3.

Table 3. Parameters of the Johnson-Cook model for Ti6Al4V (Zhang, 2011)

A, MPa	B, MPa	C	n	m	ϵ_0	T_f , °C	T_0 , °C
1098	1092	0.014	0.93	1.1	1000	1630	20

The law of contact between the surface of the cutting tool and machined surface defined by set of mechanical and thermal phenomena.

Mechanical phenomena is described by a model of friction. In our case, we assume an isotropic model of Coulomb (Bacaria, 2001):

$$|\sigma_t| \geq \mu \cdot |\sigma_n|; \quad (7)$$

$$|\sigma_t| < \mu \cdot |\sigma_n|, \quad (8)$$

where σ_t , σ_n - the components of the contact stress, μ - the friction coefficient.

The friction coefficient of titanium alloy Ti6Al4V and TiAlN PVD-coating is equal to 0.47 (Chinmaya, 2010).

Thermal effects are the distribution coefficient of the heat flux generated by friction (Pantalé, 1996). In the case of dynamic contact, problem is complicated by the fact that the boundary of contact is the source of heat. If neglect the thickness of the contact and the accumulation of heat in the contact zone, then all the heat generated by friction Φ_g will be shared between the two bodies. Introduce the concept of the distribution coefficient α , which determines the proportion of the heat flux Φ_g directed into the body 1. In our case, the body 1 is a cutting tool, and the body 2 is a material:

$$\Phi_{g \rightarrow 1} = \alpha \cdot \Phi_g; \quad (9)$$

$$\Phi_{g \rightarrow 2} = (1 - \alpha) \cdot \Phi_g. \quad (10)$$

In the simplified case where the two bodies are in perfect contact with the Vernotte ratio distribution coefficient α can be described according to the following relationship of the physical characteristics of two materials:

$$\frac{\Phi_{g \rightarrow 1}}{\Phi_{g \rightarrow 2}} = \frac{\alpha}{\alpha - 1} = \frac{\sqrt{\lambda_1 \cdot \rho_1 \cdot c_{p1}}}{\sqrt{\lambda_2 \cdot \rho_2 \cdot c_{p2}}}, \quad (11)$$

where λ_1 and λ_2 - thermal conductivity, ρ_1 and ρ_2 - density, c_{p1} and c_{p2} - specific heat cutting tool and machined material, respectively.

Thus, 32% of the heat flux generated at the contact boundary of the material and cutting plate is directed toward the material.

Take into consideration also the heat conduction coefficient for a pair of machined and the tool material. According to (Ozel, 2010) it is equal to $10^8 \text{ W} \cdot \text{m}^{-2} \cdot \text{°C}$. Assume a minimum distance of the coefficient equal to 1 μm .

2.3 Function-oriented approach in the analysis of the cutting tool loading

Currently, one of the most advanced technologies are technologies based on function-oriented approach (Михайлов, 2009). The basic signs of functionally-oriented approach are to ensure the implementation of the specified properties of products and technological actions on the following levels: the level of products, the level of components, the level of zones: macrozones, microzones, nanozones.

Theoretical and experimental research shows that the formation of chips characterized by the appearance of four zones of the loading wedge tool (Fig. 3).

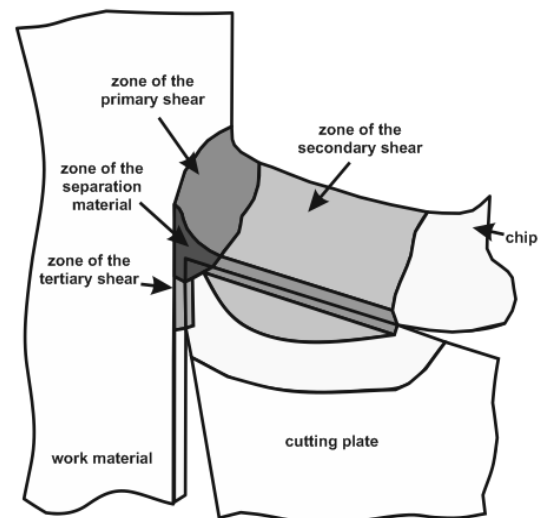


Fig. 3. Four zones of the loading wedge tool

According to the loading tool divide the working area for the following functional zones: g_1 - the contact zone of the tool with the zone of the secondary shear

(the material is moving more rapidly); g2 - the contact zone of the tool with the zone of the primary shear (produced chips, the processed material changes direction and speed - the speed of cutting to the speed of chips); g3 - contact zone of the tool with the zone of separation material (the processed material is divided into two parts by the edge tool); g4 - contact zone of the tool with the zone of the tertiary shear (friction velocity is equal to the speed of cutting).

For the analysis of physico-mechanical loading, the working part of the wedge of cutting plate is divided into subzones (1-40). The accuracy of the calculation of thermo-mechanical model increases with the number of subzones but it is limited due to requirements associated with the time of calculation, which depends on the accuracy of the model and the power of the computer. Combining subzones into functional zones of the wedge of cutting plate is shown in Fig. 4, where the parentheses are included the subzones of functional zones.

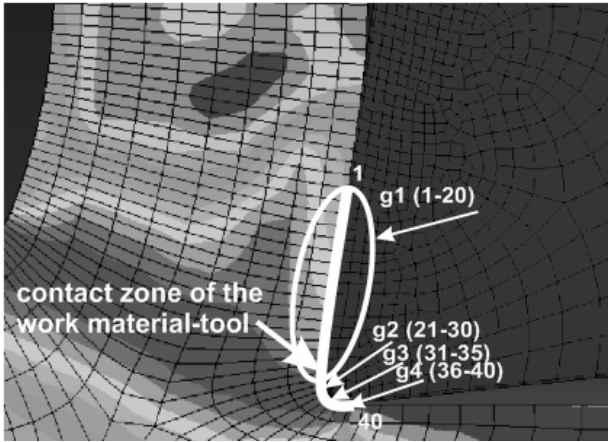


Fig. 4. Combining subzones into functional zones of the wedge of cutting plate

Thus, the overall technological action on the contact zone cutting tool and the material with respect to subzones:

$$TB = \{TB_1, TB_2, \dots, TB_i, \dots, TB_{40}\}; \quad (12)$$

$$TB = \{(\sigma_1, \tau_1, t_1); (\sigma_2, \tau_2, t_2); \dots, (\sigma_i, \tau_i, t_i), \dots, (\sigma_{40}, \tau_{40}, t_{40})\}; \quad (13)$$

where σ_i - contact pressure of i - subzone, τ_i - contact shear of i - subzone, t_i contact temperature of i -subzone.

After the unification of subzones in functional zones of the wedge of cutting plate:

$$TB = \{M[TB_{1-20}], M[TB_{21-30}], M[TB_{31-35}], M[TB_{36-40}]\}; \quad (14)$$

$$TB = \{M[\sigma_{1-20}, \tau_{1-20}, t_{1-20}], M[\sigma_{21-30}, \tau_{21-30}, t_{21-30}], M[\sigma_{31-35}, \tau_{31-35}, t_{31-35}], M[\sigma_{36-40}, \tau_{36-40}, t_{36-40}]\}. \quad (15)$$

Physical and mechanical loading of functional zones of the wedge of cutting plate are presented in the table 4.

Table 4. Physical and mechanical loading of functional zones of the wedge of cutting plate for machining Ti6Al4V

physical and mechanical loading	functional zones of the wedge of cutting plate			
	g1	g2	g3	g4
cutting conditions vc65f03ae3				
contact pressure, MPa	117	2776	1958	3240
contact shear MPa	53	8	30	75
contact temperature, °C	848	884	846	864
cutting conditions vc90f03ae3				
contact pressure, MPa	110	2229	2543	2138
contact shear MPa	31	12	51	16
contact temperature, °C	864	931	892	922
cutting conditions vc115f03ae3				
contact pressure, MPa	114	1708	2776	3527
contact shear MPa	31	9	72	39
contact temperature, °C	913	948	946	958

2.4 Technological methods to increase the strength of the cutting tool

The basic technological methods of increasing the strength of cutting tools are: an optimization of cutting conditions, a choice of structure and properties of coatings for carbide tools, an use of technology intensifies the process of cutting: a cutting fluid, a ultrasound, a laser technology, etc.

For effective selection process of the method and its parameters need to know its effect on physico-mechanical loading of functional zones of the wedge of cutting plate. For this construct interpolated graphs of dependencies of physical and mechanical loading of functional zones of the wedge of cutting plate of technological parameters of the considered method.

Therefore necessary select one of the structural variants of technological action for increasing the strength of carbide tools coated.

2.5 Functionally-oriented optimization of the cutting speed

As an example, consider a functional-oriented optimization of the cutting speed for machining titanium alloy Ti6Al4V. As a base regime, we take the cutting conditions vc65f03ae3. The purpose of this optimization is to determine the cutting conditions with a maximum cutting speed (for maximum productivity) without increasing the total load on the tool. The first step is to analyze the physical and mechanical loading parameters (contact pressure, contact shear and contact temperature) of functional zones of the wedge of cutting plate.

By interpolating the data previously submitted

thermomechanical models of the cutting process were obtained depending on the cutting speed of the physical and mechanical loading parameters of functional zones of the wedge of cutting plate. Effect of cutting speed on the contact pressure in functional zones of the wedge of cutting plate is shown in figure 5.

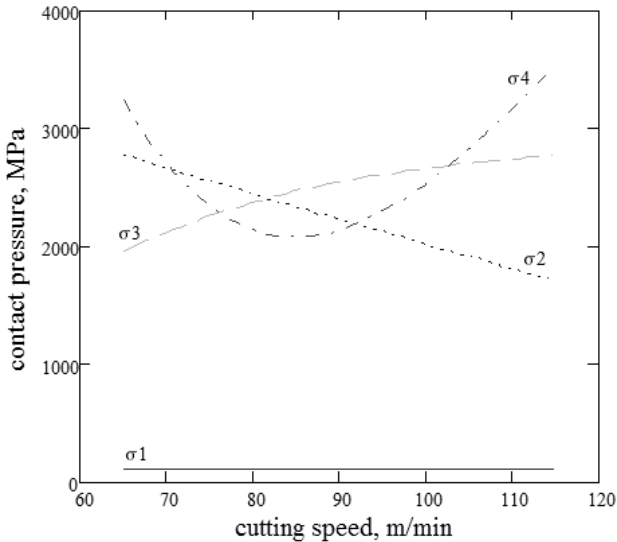


Fig. 5. Effect of cutting speed on the contact pressure in functional zones of the wedge of cutting plate for machining Ti6Al4V, (σ_1 , σ_2 , σ_3 , σ_4 - contact pressure in g_1 , g_2 , g_3 , g_4 respectively)

Effect of cutting speed on the contact shear in functional zones of the wedge of cutting plate is shown in figure 6.

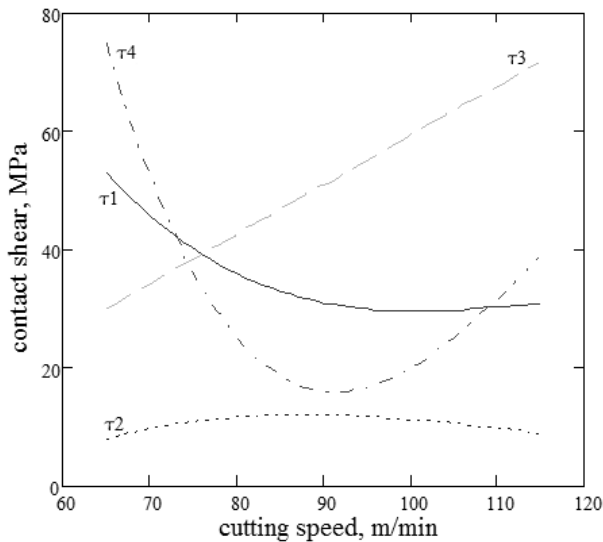


Fig. 6. Effect of cutting speed on the contact shear in functional zones of the wedge of cutting plate for machining Ti6Al4V, (τ_1 , τ_2 , τ_3 , τ_4 - contact shear in g_1 , g_2 , g_3 , g_4 respectively)

Effect of cutting speed on the contact temperature in functional zones of the wedge of cutting plate is shown in figure 7.

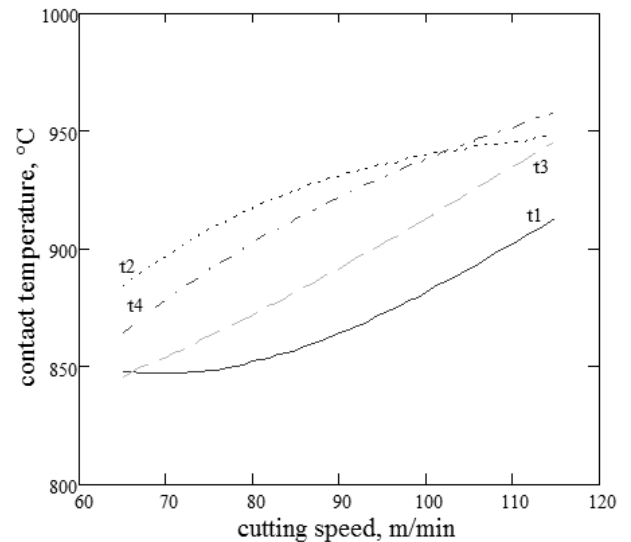


Fig. 7. Effect of cutting speed on the contact temperature in functional zones of the wedge of cutting plate for machining Ti6Al4V, (t_1 , t_2 , t_3 , t_4 - contact temperature in g_1 , g_2 , g_3 , g_4 respectively)

In terms of contact pressure, the optimal value of the cutting speed is at the intersection graphs of functions σ_2 and σ_3 in the zone of minimum values of σ_4 and corresponds to 82 m/min, the contact shear - corresponds to the minimum of τ_4 - 95 m/min.

For all functional zones of the wedge cutting plate contact temperature increases with increasing speed, but for each zone, this function is different.

The second step is the synthesis of the physical and mechanical loading parameters (contact pressure, contact shear and contact temperature) of functional zones of the wedge of cutting plate.

Define the change in the overall loading of the cutting plate relative to the base regime $vc65f03ae3$ as follows:

$$A(v) = \sum_{i=1}^4 \left(\frac{\sigma_i - \sigma'_i}{\sigma'_i} + \frac{\tau_i - \tau'_i}{\tau'_i} + \frac{t_i - t'_i}{t'_i} \right) \cdot 100\%, \quad (16)$$

where v - cutting speed, m/min; σ_i - contact pressure for i - functional zones of the wedge of cutting plate, MPa; τ_i - contact shear for i - functional zones of the wedge of cutting plate, MPa; t_i - contact temperature for i - functional zones of the wedge of cutting plate °C; σ'_i - contact pressure of the base regime for i - functional zones of the wedge of cutting plate, MPa; τ'_i - contact shear of the base regime for i - functional zones of the wedge of cutting plate, MPa; t'_i - contact temperature of the base regime for i - functional zones of the wedge of cutting plate, °C.

This function of the change in the overall loading of the cutting plate relative to the base regime $vc65f03ae3$ and line of the base regime are presented in figure 8.

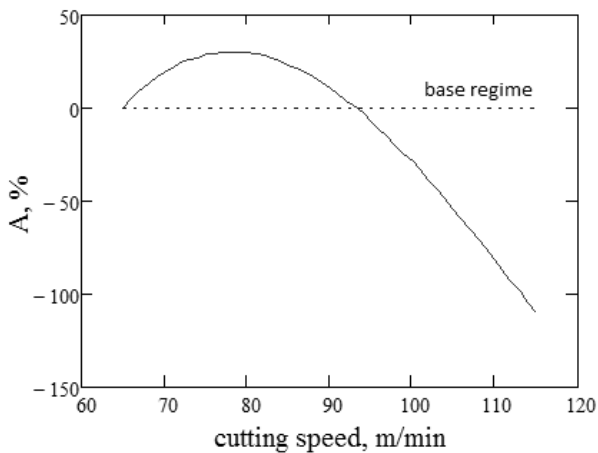


Fig. 8. Change in the overall loading on the cutting plate relative to the base regime

Thus, the maximum cutting speed, which does not cause the total loading of the cutting plate above the basic regime, located at the intersection of the zero value (a function corresponds to the basic regime) and the function changes the overall loading of cutting plate corresponds to the cutting speed 93m/min.

3. CONCLUSIONS

The presented method of analysis of physico-mechanical loading parameters by means of functional-oriented approach and thermo-mechanical simulation of the cutting process makes it possible to adapt the technological actions (cutting conditions, structure and properties of coatings technology intensification: cutting fluids, ultrasound, cutting, laser etc.) to the operating characteristics of various functional zones of the wedge of cutting plate. This analysis allowed increasing the cutting speed of 1.43 times without increasing the overall load on the cutting plate.

4. REFERENCES

1. Bacaria, J.-L., (2001). *Un modèle comportemental et transitoire pour la coupe des métaux*, pp. 34-39, Ph.D. Thesis, ENI de Tarbes.
2. Braham Bouchnak, T., (2010). *Etude du comportement en sollicitations extrêmes et de l'usinabilité d'un nouvel alliage de titane aéronautique: le Ti555-3*, pp. 45-54, Ph.D. Thesis, ENSAM d'Angers.
3. Chinmaya, R., Dandekar, C.R., Shin, Y.C., Barnes, J., (2010). *Machinability improvement of titanium alloy (Ti-6Al-4V) via LAM and hybrid machining*, International Journal of Machine Tools & Manufacture, 50, pp. 174-182.
4. Gökçaya, H., Nalbant, M., Yaşar, M., (2009). *Kaplama çeşidi-katman sayısı ve sıcaklığa bağlı olarak kesici takım üst yüzeyindeki takım-talaş temas alan bölgesi ve yanak yüzeyindeki sıcaklık dağılımının sonlu elemanlarla analizi*, Available

from

http://iats09.karabuk.edu.tr/press/bildiriler_pdf/IATS_09_05-99_1071.pdf, Accessed: 08/01/2012.

5. Jianxin, D., (2008). *Diffusion wear in dry cutting of Ti-6Al-4V with WC/Co carbide tools*, Wear, 265, pp. 1776-1783.
6. Kalay, F., (2006). *Simulation numérique de l'usinage Application à l'aluminium AU4G (A2024-T351)*, Available from <http://www.techniques-ingenieur.fr/base-documentaire/mecanique-th7/travail-des-materiaux-assemblage-ti153/simulation-numerique-de-l-usinage-bm7002>, Accessed: 08/01/2012.
7. Kamnis, S., Gua, S., Lu, T.J., Chen, C., (2008). *Computational simulation of thermally sprayed WC-Co powder*, Phys.: Computational Materials Science, 43, pp. 1172-1182.
8. Kay, G., (2003). *Failure modeling of titanium 6Al-4V and aluminum 2024-T3 with the Johnson-Cook material model*, Technical report DOT/FAA/AR-03/57. Available from <http://www.tc.faa.gov/its/worldpac/techrpt/ar03-57.pdf>, Accessed: 08/01/2012.
9. Okamoto, S., Nakazono, Y., Otsuka, K., Shimoitani, Y., Takada, J., (2005). *Mechanical properties of WC/Co cemented carbide with larger WC grain size*, Materials Characterization, 55, pp. 281-287.
10. Ozel, T., Sima, M., Srivastava, A.K., Kaftanoglu, B., (2010). *Investigations on the effects of multi-layered coated inserts in machining Ti-6Al-4V alloy with experiments and finite element simulations*, CIRP Annals - Manufacturing Technology, 59, pp. 77-82.
11. Pantalé, O., (1996). *Modélisation et simulation tridimensionnelles de la coupe des métaux*, Ph.D. Thesis, pp. 45-56, Université de Bordeaux I.
12. Pantalé, O., (2005). *Plateforme de prototypage virtuel pour la simulation numérique en grandes transformations thermomécaniques rapides: habilitation à diriger des recherches*, Available from <http://tel.archives-ouvertes.fr/docs/00/04/83/19/PDF/tel-00009913.pdf>, Accessed: 08/01/2012.
13. Staia, M.H., D'Alessandria, M., Quinto, D.T., Roudet, F., Astort, M.M., (2006). *High-temperature tribological characterization of commercial TiAlN coatings*, Phys.: Condens. Matter, 18, pp. 1727-1736.
14. Zhang, Y., Sima, M., Srivastava, A.K., Kaftanoglu, B., (2011). *FE-model for Titanium alloy (Ti-6Al-4V) cutting based on the identification of limiting shear stress at tool-chip interface*, International journal of material forming, 4(1), pp. 11-23.